Rab9-dependent retrograde transport and endosomal sorting of the endopeptidase furin

Pei Zhi Cheryl Chia, Isabelle Gasnereau, Zi Zhao Lieu and Paul A. Gleeson*

The Department of Biochemistry and Molecular Biology and Bio21 Molecular Science and Biotechnology Institute, The University of Melbourne, Victoria 3010, Australia

*Author for correspondence (pgleeson@unimelb.edu.au)

Accepted 20 March 2011
Journal of Cell Science 124, 2401-2413

doi:10.1242/jcs.083782

Summary

The endopeptidase furin and the *trans*-Golgi network protein TGN38 are membrane proteins that recycle between the TGN and plasma membrane. TGN38 is transported by a retromer-dependent pathway from early endosomes to the TGN, whereas the intracellular transport of furin is poorly defined. Here we have identified the itinerary and transport requirements of furin. Using internalisation assays, we show that furin transits the early and late endosomes en route to the TGN. The GTPase Rab9 and the TGN golgin GCC185, components of the late endosome-to-TGN pathway, were required for efficient TGN retrieval of furin. By contrast, TGN38 trafficking was independent of Rab9 and GCC185. To identify the sorting signals for the early endosome-to-TGN pathway, the trafficking of furin–TGN38 chimeras was investigated. The diversion of furin from the Rab9-dependent late-endosome-to-TGN pathway to the retromer-dependent early-endosome-to-TGN pathway required both the transmembrane domain and cytoplasmic tail of TGN38. We present evidence to suggest that the length of the transmembrane domain is a contributing factor in endosomal sorting. Overall, these data show that furin uses the Rab9-dependent pathway from late endosomes and that retrograde transport directly from early endosomes is dependent on both the transmembrane domain and the cytoplasmic tail.

Key words: Furin, Retrograde transport, Rab9, TGN38, Endosomal sorting, Retromer

Introduction

Recycling of membrane proteins between the cell surface and intracellular endosomes is a feature of many membrane molecules, such as the transferrin receptor. A subset of these recycling proteins have a more complex itinerary and can be transported from endosomes to the *trans*-Golgi network (TGN), by a process known as retrograde transport. Recycling proteins that use retrograde transport pathways include sorting receptors such as the mannose-6-phosphate receptor (M6P-R), sortilin and Wntless, the transmembrane proteins TGN38 and TGN46, furin and SNAREs and ion and glucose transporters (Ghosh et al., 1998; Ghosh et al., 2003; Shewan et al., 2003; Sandvig and van Deurs, 2005; Bonifacino and Rojas, 2006; Johannes and Popoff, 2008). In addition, bacterial and plant toxins, such as Shiga toxin, cholera toxin, pertussis toxin and ricin are known to hijack retrograde transport pathways to mediate toxicity (Sandvig and van Deurs, 2000; Utskarpen et al., 2006; Plaut and Carbonetti, 2008). Both endogenous and exogenous cargoes have been instrumental in delineating the identity of the distinct retrograde pathways (Johannes and Popoff, 2008; Lieu and Gleeson, 2011), which include transport pathways from the early and recycling endosomes to the TGN, used by the Shiga and cholera toxins and TGN38, and the v-SNARE VAMP4 (Ghosh et al., 1998; Mallard et al., 1998; Tran et al., 2007) and a pathway from the late endosome to the TGN, used by M6P-R (Mallet and Maxfield, 1999; Barbero et al., 2002).

Furin is an essential endopeptidase of the proprotein convertase family whose primary role is to cleave the proprotein domains of immature proteins, thus triggering their enzymatic activation. Notable amongst its substrates are β-nerve growth factor (β-NGF), members of the tumour growth factor-β (TGF-β) family, and bone morphogenetic protein-4 (BMP-4), and the α- and β-secretases associated with Alzheimer's disease (Cui et al., 1998; Bennett et al., 2000; Dubois et al., 2001; Lopez-Perez et al., 2001). Furin cleavage of these substrates occurs at the TGN but is not limited to this compartment. Cell-surface activation of the anthrax toxin is an obligatory step in pore-formation at cellular membranes (Molloy et al., 1992), whereas early-endosomal furin is required for the liberation of the active domain of A/B-type toxins such as *Pseudomonas* endotoxin A and Shiga toxin (Molloy et al., 1999). The detection of furin activity at various cellular compartments reinforces furin as a bona fide recycling protein that cycles between the cell surface and the TGN via endosomes. An early study by Mallet and Maxfield, using a Tac–furin chimera consisting of the cytoplasmic domain of furin and the transmembrane and lumenal domains of the Tac antigen, proposed that furin is delivered to the TGN via late endosomes (Mallet and Maxfield, 1999). These authors also showed that the retrograde transport of a Tac-TGN38 chimera was transported from the early or recycling endosome en route to the TGN. More recent studies have confirmed the movement of TGN38 directly from the early endosomes to the TGN, thereby bypassing the late endosomal compartment (Banting and Ponnambalam, 1997; Lieu and Gleeson, 2010).

It has become increasingly clear that the different retrograde pathways are characterised by different sets of machinery. In particular, the retromer complex functions as an endosomal coat protein that mediates the early endosomal retrograde transport of a number of cargoes such as the cation-independent mannose-6-phosphate receptor (CI-M6P-R), Wntless, Shiga toxin, polymeric immunoglobulin receptors and TGN38 (Arighi et al., 2004; Seaman, 2004; Verges et al., 2004; Popoff et al., 2007; Belenkaya et al., 2008; Franch-Marro et al., 2008; Port et al., 2008; Yang et al.,

Journal of Cell Science

2008; Lieu and Gleeson, 2010). Retromer is comprised of two subcomplexes: a cargo recognition trimer consisting of Vps26–Vps35–Vps29 and a sorting nexin (SNX) dimer that contains the PX and Bar domains that bind lipids to initiate membrane tubulation (Carlton et al., 2004; Seaman, 2005; Rojas et al., 2007). The sorting nexin dimer is thought to consist of SNX1 and SNX2, both of which can independently bind to the recognition subcomplex, but might also dimerise with SNX5 and SNX6, perhaps adding another level of specificity in cargo selection (Rojas et al., 2007; Wassmer et al., 2009). Distinct SNARE (soluble *N*-ethylmaleimide-sensitive factor attachment protein receptor) complexes are associated with either the early- or late-endosomal-to-TGN pathway. Two SNARE complexes are involved in the transport from early or recycling endosomes to the TGN: a SNARE complex consisting of the t-SNAREs syntaxin-16, syntaxin-6 and Vti1a with the v-SNARE VAMP4 (or VAMP3) (Mallard et al., 2002), the other made up of the t-SNAREs syntaxin-5, GS28 and Ykt6, which pairs with the v-SNARE GS15 (Xu et al., 2002). For the late-endosomal-to-TGN route, a syntaxin-10 complex comprised of syntaxin-10, syntaxin-16, Vti1a and VAMP3 appears to be required (Ganley et al., 2008). Tethering machinery, in particular golgins at the TGN, further differentiate the two retrograde routes (Goud and Gleeson, 2010). These TGN golgins are peripheral membrane proteins recruited to the TGN by the GRIP domain, a C-terminal targeting sequence (Barr, 1999; Kjer-Nielsen et al., 1999a; Munro and Nichols, 1999), and have an extensive coiled-coil structure typical of tethers involved in docking of incoming vesicles. The TGN golgin, GCC88, is essential for the efficient retrograde transport of TGN38 from the early endosomes (Lieu et al., 2007), whereas GCC185 is involved in the tethering of M6P-R-carrying vesicles emanating from the late endosomes (Reddy et al., 2006; Ganley et al., 2008). The tethering function of GCC185 is dependent on its interaction with the late endosome-localised Rab GTPase Rab9. Rab9 has been detected on transport vesicles before fusion with the TGN and moreover, was found to be required for endosome-to-TGN transport of M6P-Rs (Lombardi et al., 1993; Barbero et al., 2002).

Although the early-endosome-to-TGN and the late-endosome-to-TGN retrograde pathways are defined on the basis of the trafficking machinery and cargoes, relatively little is known about the targeting signals of the cargo proteins that define their specific retrograde transport routes. Discrete sorting motifs in the cytoplasmic tails of recycling proteins have been shown to be required for the endocytosis and TGN-retrieval of these cargos. For example, Yxxϕ motifs in TGN38 and furin cytoplasmic tails are required for their internalisation (Bos et al., 1993; Humphrey et al., 1993; Wong and Hong, 1993; Marks et al., 1997; Teuchert et al., 1999), Ser331 is important as a TGN-retrieval signal in TGN38 (Roquemore and Banting, 1998), whereas the acidic cluster EECPSDSEEDE is required for the TGN retrieval of furin (Voorhees et al., 1995). Although the importance of these motifs in endocytosis and TGN retrieval have been identified, nonetheless it is not clear how signals contribute to the endosomal sorting events of these membrane proteins.

Here we have defined the itinerary and retrograde transport requirements of furin and show that furin is transported by the Rab9-dependent late-endosome-to-TGN pathway. We have exploited the distinct retrograde transport routes of furin and TGN38 to dissect the requirements for selective transport along the two retrograde transport pathways. The findings presented here show that the choice of retrograde pathway en route to the TGN not only requires the cytoplasmic domain, but is also dependent on information inherent in the transmembrane region.

Results

Intracellular itinerary of Furin

Furin cycles between the TGN and the cell surface (Thomas, 2002) and previous studies with chimeras indicated that furin might be delivered to the TGN through the late endosomes (Mallet and Maxfield, 1999). To define the intracellular itinerary of wild-type full-length furin, we tracked the transport of furin from the plasma membrane to the Golgi by an internalisation assay. HeLa cells were transfected with a FLAG-tagged furin construct and transfected cells were incubated with anti-FLAG antibodies on ice. As expected, the antibody–furin complexes were restricted to the cell surface at 4°C (Fig. 1A, 0 minutes). Surface-bound antibody–

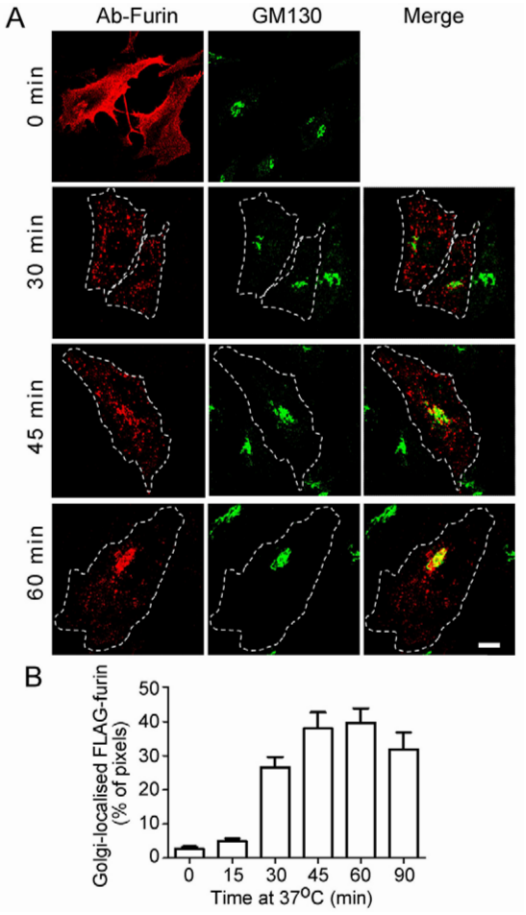

Fig. 1. Trafficking of full-length furin from the plasma membrane to Golgi. (**A**) HeLa cells were transfected with FLAG–furin for 24 hours. Monolayers were incubated with anti-FLAG antibodies for 45 minutes on ice, washed in PBS, and either fixed (0 min) or incubated in serum-free medium for up to 90 minutes at 37°C to internalise the antibody–FLAG–furin complexes. Immediately following the incubation, monolayers were fixed and permeabilised and stained with Alexa-Fluor-568-conjugated anti-rabbit IgG (red). GM130 was stained with mouse monoclonal anti-GM130 antibodies, followed by Alexa-Fluor-488-conjugated anti-mouse IgG (green). Scale bar: 10 µm. (**B**) The number of FLAG–furin (red) pixels within the GM130-marked region was expressed as a percentage (±s.e.m.) of the total number of FLAG–furin pixels within each cell using the plug-in OBCOL on the ImageJ program (n=20 for each time point).

furin complexes were then internalised at 37°C over a 90-minute period. Antibody–FLAG–furin complexes were efficiently internalised; by 30 minutes, the surface furin had been internalised and located in endosomal structures distributed in the cell periphery and throughout the cytoplasm. By 45 minutes, the majority of the internalised FLAG–furin complexes were found concentrated in the perinuclear region, which overlapped with the *cis*-Golgi marker GM130, and some was detected in endosomal structures. By 60 minutes of internalisation, a substantial amount of the internalised furin colocalised with the Golgi marker (Fig. 1A).

The kinetics of arrival at the Golgi was determined by quantifying the number of FLAG–furin-positive pixels located within the GM130-defined Golgi region. Very little internalised furin was detected within the Golgi after 15 minutes of internalisation; subsequently there was a dramatic increase in the arrival of furin at the Golgi. By 45 minutes, ~40% of the total intracellular FLAG–furin pixels were localised within the Golgi region (Fig. 1B). Pixel overlap with organelle markers provides a convenient measure of intracellular distribution; however, it is likely to be an underestimate of absolute amount of furin that has been transported to the Golgi, because it does not take into account pixel intensity.

The endosomal structures containing internalised furin were identified using the endosome-specific markers EEA1, CD63 and Rab11. By 15 minutes of internalisation, the majority of the furin-positive endosomal structures were EEA1 positive (Fig. 2A) and 40% of the total intracellular FLAG–furin pixels overlapped with EEA1 (Fig. 2C). Subsequently the level of furin in the early endosomes waned to around 30% of the total internalised pixel pool at later time points. The localisation of FLAG–furin with the late endosome marker CD63 showed an increase over the 45 minutes to >40% of the total internalised furin (Fig. 2B,D). The increase in the late endosomal pool of internalised furin from 15 to 30 minutes indicates that furin is sequentially moving from the early endosome to the late endosome. By contrast, only a low level of overlap was observed between FLAG–furin and the recycling endosome marker GFP–Rab11, after either 15 minutes or 45 minutes of internalisation (supplementary material Fig. S1A). The recycling endosome can be difficult to resolve from the Golgi in HeLa cells, hence we also examined the intracellular location of furin in transfected CHO cells, where the recycling endosome can be more readily resolved. We marked the recycling endosome in CHO cells by expressing GFP–Rab11, which showed a typical tight perinuclear location very distinct from GM130-stained

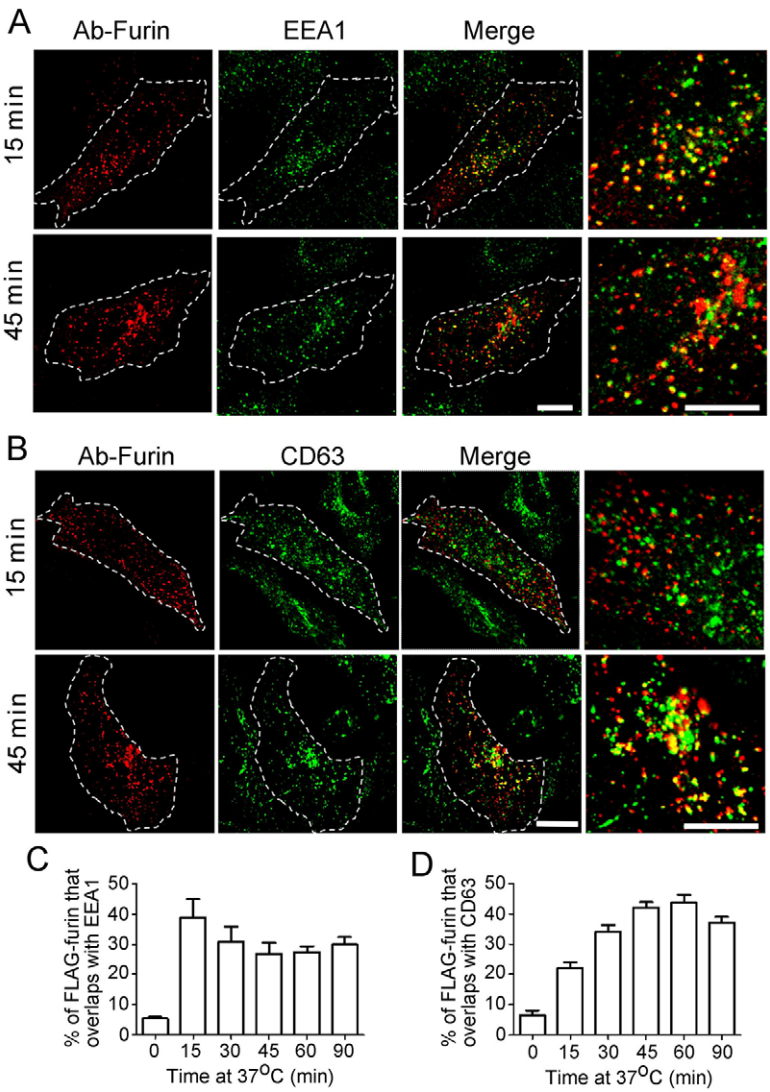

Fig. 2. Furin is transported via the early and late endosomes en route to the TGN. HeLa cells were transfected with FLAG–furin for 24 hours and monolayers were incubated with anti-FLAG antibodies for 45 minutes on ice. Cells were washed in PBS and incubated in serum-free medium for 15 or 45 minutes at 37°C, then fixed, permeabilised and stained for internalised antibody–FLAG–furin complexes with Alexa-Fluor-568-conjugated anti-rabbit IgG (red) and for (**A**) EEA1 using mouse monoclonal anti-EEA1 antibodies (green) or (**B**) CD63 using mouse monoclonal anti-CD63 antibodies (green). Scale bars: 10 µm. The number of FLAG–furin pixels that overlapped with (**C**) EEA1 or (**D**) CD63 was expressed as a percentage (±s.e.m.) of the total number of FLAG–furin pixels within each cell using the plug-in OBCOL on the ImageJ program (n=20 for each time point).

structures. After 45 minutes of FLAG–furin internalisation, the antibody–furin complexes were detected as a ring of structures around the Rab11-positive compartment with almost no overlap between furin and Rab11 (supplementary material Fig. S1B). Furthermore, quantitative analyses over an extended period of furin internalisation revealed that the overlap between furin and GFP–Rab11 did not increase throughout the period of internalisation (supplementary material Fig. S1B). These data confirm that in more than one cell type, the majority of furin does not traffic to the recycling endosomes.

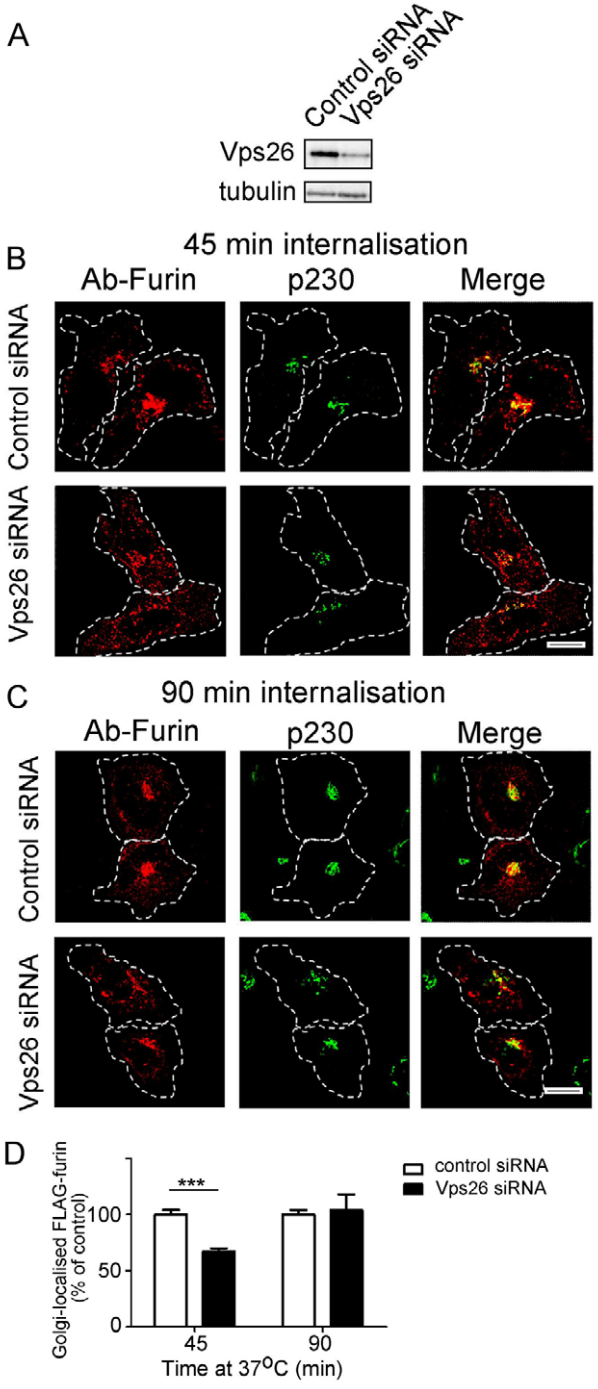

Retrograde transport of furin is Rab9 dependent and retromer independent

Because furin traverses the early and the late endosomes, it is possible that it is transported to the TGN from one or both these endosomal compartments. To distinguish between these possibilities, we analysed the requirement of various machinery components of the early-endosome-to-TGN and the late-endosome-to-TGN pathway for furin transport. Retromer has been shown to regulate retrograde transport of a number of cargos from the early endosomes (Bujny et al., 2007; Popoff et al., 2007; Utskarpen et al., 2007) and initially we assessed whether retromer is required for retrograde transport of furin. Retromer comprises two sub-complexes: a cargo recognition trimer of Vps26–Vps35–Vps29 and a sorting nexin (SNX) dimer. The retromer component Vps26 was silenced in HeLa cells using a previously characterised human Vps26 siRNA target sequence (Arighi et al., 2004; Popoff et al., 2007). Immunoblotting (Fig. 3A) and immunofluorescence (not shown) showed that the protein level of Vps26 was reduced by >85% in the *VPS26* siRNA-transfected cell population. Depletion of Vps26 resulted in some fragmentation of the Golgi (Fig. 3B,C), as previously reported (Seaman, 2004; Lieu and Gleeson, 2010), and immunofluorescence revealed that after 45 minutes of internalisation, there was a reduced level of Golgi-localised furin, compared with cells treated with control siRNA (Fig. 3B). However, by 90 minutes, there was no difference in the Golgi-localised furin between Vps26-depleted and control cells (Fig. 3C,D), suggesting that the reduction of Vps26 had only a minor effect on the retrograde transport of furin. We also assessed the requirement of two sorting nexins that are components of retromer, namely SNX1 and SNX2. Silencing of *SNX1* also resulted in Golgi fragmentation and the kinetics of furin transport was similar to Vps26-depleted cells, i.e. a reduced level of Golgi-localised furin after 45 minutes of internalisation, but no difference in Golgi-localised furin at 90 minutes compared with cells treated with control siRNA (supplementary material Fig. S2). The slower rate of retrieval of furin to the Golgi in Vps26- and SNX1-depleted cells probably reflects a reduced efficiency of transport to a fragmented Golgi, nonetheless the effect is relatively minor. Silencing of *SNX2* had no apparent effect on the retrograde transport of furin (supplementary material Fig. S3). By contrast, and as expected, the

Fig. 3. Retrograde transport of furin does not require Vps26. HeLa cells were transfected with either control siRNA or siRNA to knockdown Vps26 for 48 hours and transfected again with FLAG–furin for a further 24 hours. (**A**) For immunoblotting, cells were lysed in SDS-PAGE reducing buffer and cell extracts were subjected to SDS-PAGE on a 4–12% gradient polyacrylamide gel. Proteins were transferred to a PVDF membrane and probed with rabbit anti-Vps26 antibodies using a chemiluminescence detection system. The membrane was then stripped and reprobed with mouse anti-α-tubulin antibodies. (**B**,**C**) For internalisation assays, transfected cells were incubated with mouse anti-FLAG antibodies for 45 minutes on ice. Monolayers were washed in PBS and incubated in serum-free medium for (B) 45 minutes or (C) 90 minutes at 37°C and then fixed and permeabilised. These were stained for the internalised antibody–FLAG–furin complexes with Alexa-Fluor-568-conjugated anti-mouse IgG (red) and for p230 using rabbit anti-p230 antibodies, followed by Alexa-Fluor-488-conjugated anti-rabbit IgG (green). Scale bars: 10 µm. (**D**) Quantification of FLAG–furin levels within the Golgi of siRNA-treated cells. The percentage (±s.e.m.) of the total FLAG–furin pixels that overlapped with p230 in each cell was determined using the plug-in OBCOL on ImageJ (n=20 for each time-point). The data from Vps26-knockdown cells is expressed as a percentage of the control siRNA data set. ***P<0.001.

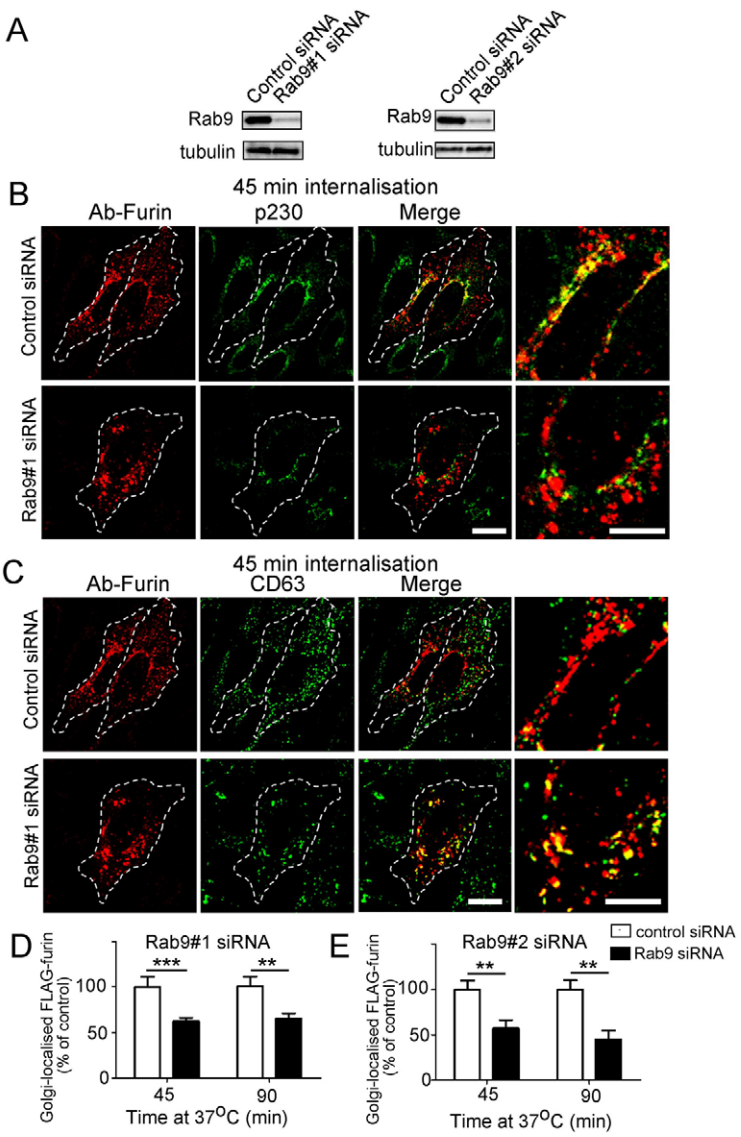

Fig. 4. Retrograde transport of furin is dependent on Rab9. HeLa cells were transfected with either control siRNA, Rab9#1 siRNA or Rab9#2 siRNA, as indicated, for 48 hours and transfected again with FLAG–furin for a further 24 hours. (**A**) For immunoblotting, cells were lysed in SDS-PAGE reducing buffer and cell extracts were subjected to SDS-PAGE on a 4–12% gradient polyacrylamide gel. Proteins were transferred to a PVDF membrane and probed with mouse anti-Rab9 antibodies using a chemiluminescence detection system. The membrane was then stripped and reprobed with mouse anti-α-tubulin antibodies. For internalisation assays, transfected cells were incubated with rabbit anti-FLAG antibodies for 45 minutes on ice. Cells were washed in PBS and incubated in serum-free medium for 45 minutes or 90 minutes at 37°C and then fixed and permeabilised. These were stained for the internalised antibody-bound FLAG-furin with Alexa-Fluor-568-conjugated anti-rabbit IgG (red) and **(B)** p230 using human anti-p230 antibodies followed by Alexa-Fluor-647-conjugated anti-human IgG (pseudo-coloured green) or **(C)** CD63 using mouse monoclonal anti-CD63 antibodies, followed by Alexa-Fluor-488-conjugated anti-IgG (green). Scale bars: 10 µm. Quantification of FLAG-furin levels within the Golgi of cells treated with (**D**) Rab9#1 siRNA and (**E**) Rab9#2 siRNA. The percentage of the total FLAG–furin pixels that overlapped with p230 in each cell was determined using the plug-in OBCOL on ImageJ (n=20 for each time-point). The data from Rab9-knockdown cells is expressed as a percentage of the control siRNA data set (±s.e.m.). ***P<0.001; **P<0.01.

retrograde transport of the cargo TGN38, which traffics from the early endosome to the TGN, was reduced in Vps26-depleted cells and SNX2-depleted cells, but not SNX1-depleted cells over a 120-minute period at 37°C (supplementary material Fig. S5A–C). Fluorescence analyses showed that there was significant reduction (~50%) in the level of Golgi-localised TGN38-antibody complexes in Vps26-depleted or SNX2-depleted cells compared with control cells at 60 minutes or 120 minutes of internalisation (supplementary material Fig. S5A,C). Thus, TGN38 is dependent on the retromer components Vps26 and SNX2 for endosome-to-TGN transport, whereas furin transport does not require retromer.

Rab9 has been shown to be an essential component for the retrograde transport of the M6P-R along the late-endosome-to-TGN pathway (Lombardi et al., 1993; Barbero et al., 2002). *RAB9* was silenced in HeLa cells using previously characterised human *RAB9* siRNA target sequences and immunoblotting demonstrated a reduction of >85% of Rab9 (Fig. 4A) in transfected HeLa cells. In Rab9-depleted cells there was a substantial increase in the percentage of internalised antibody-furin complexes that remained located at endosomal structures for extended periods compared with control siRNA cells (Fig. 4B). Quantification of Golgi-localised furin, showed that there was a ~40% reduction in furin transported to the Golgi compared with control cells at either 45 minutes or 90 minutes of internalisation (Fig. 4D). Silencing of *RAB9* with a second *RAB9* siRNA target sequence gave similar results, with a >50% reduction in furin transported to the Golgi after 90 minutes of internalisation compared with control cells (Fig. 4E). Consistent with the reduced levels of Golgi-localised furin in Rab9-depleted cells was a more extensive colocalisation of furin with the late endosome marker CD63 (percentage overlap of FLAG–furin with CD63 at 45 minutes: control cells, 42.6±3.6%; Rab-depleted cells, 50.6±9.3%; P=0.03) indicating a reduction in the transport of furin out of the late endosome in Rab9-depleted cells.

Another component that is required for late endosome-to-TGN transport is the TGN golgin GCC185. Depletion of GCC185 resulted in extensive fragmentation of the Golgi, as reported previously (Derby et al., 2007). Significantly, there was a substantial reduction in antibody–furin complexes detected at the Golgi fragments of GCC185-depleted cells (Fig. 5), with a 45% and 35%

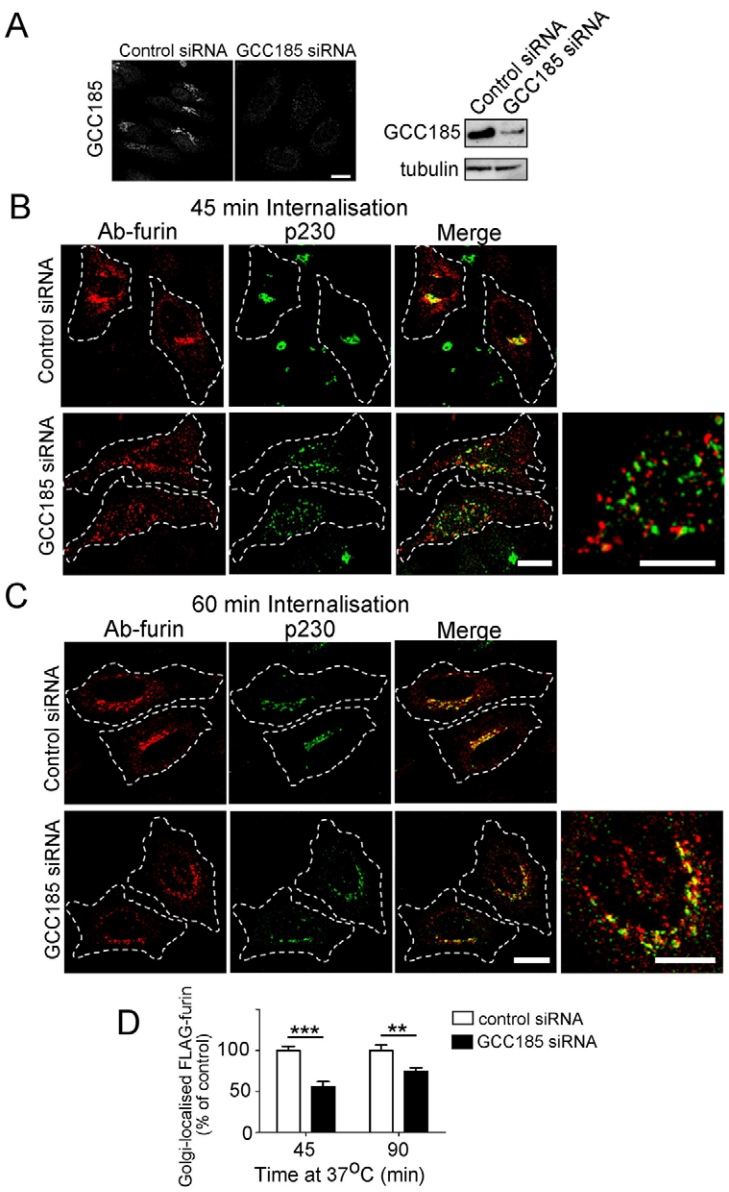

Fig. 5. Furin requires the TGN golgin GCC185 for retrograde transport. HeLa cells were transfected with either control siRNA or siRNA against mRNA encoding GCC185 for 48 hours and transfected again with FLAG–furin for a further 24 hours. (**A**) Endogenous GCC185 was stained with affinity-purified rabbit anti-GCC185 antibodies, followed by Alexa-Fluor-568-conjugated anti-rabbit IgG. For immunoblotting, cells were lysed in SDS-PAGE reducing buffer and cell extracts were subjected to SDS-PAGE on a 4–12% gradient polyacrylamide gel. Proteins were transferred to a PVDF membrane and probed with affinity-purified rabbit anti-GCC185 antibodies using a chemiluminescence detection system. The membrane was then stripped and reprobed with mouse anti-α-tubulin antibodies. For internalisation assays, transfected cells were incubated with mouse monoclonal anti-FLAG antibodies for 45 minutes on ice. Cells were washed in PBS and incubated in serum-free medium for (**B**) 45 minutes or (**C**) 90 minutes at 37°C and then fixed and permeabilised. Monolayers were stained for the internalised antibody-bound FLAG–furin with Alexa-Fluor-568-conjugated anti-mouse IgG (red) and for p230 using rabbit anti-p230 antibodies, followed by Alexa-Fluor-488-conjugated anti-rabbit IgG (green). Scale bars: 10 μm. (**D**) Quantification of FLAG–furin levels within the Golgi of GCC185-knockdown cells. The percentage of the total FLAG–furin pixels that overlapped with p230 in each cell was determined using the plug-in OBCOL on ImageJ (n=20 for each time point). The data from GCC185-knockdown cells are expressed as a percentage (±s.e.m.) of the control siRNA data set. $^{**}P<0.01$; $^{***}P<0.001$.

reduction in Golgi trafficking of the furin at 45 minutes and 90 minutes of internalisation, respectively (Fig. 5D). By contrast, the retrograde transport of TGN38 was unaffected by the knockdown of GCC185 (supplementary material Fig. S5E).

The t-SNAREs syntaxin-10, syntaxin-16 and Vti1a are required for the transport of M6P-R along the late endosome to TGN route (Ganley et al., 2008). Depletion of either syntaxin-10 or syntaxin-16, but not syntaxin-6, resulted in a reduction in antibody–furin complexes detected within the Golgi region (supplementary material Fig. S4), again consistent with the transport of furin along the Rab9-dependent pathway. However, and as expected, knockdown of syntaxin-10 had no effect on TGN38 transport (supplementary material Fig. S5F).

Diversion of the retrograde trafficking of furin from a Rab9-dependent pathway to a retromer-dependent pathway

As discussed earlier, a variety of signals have been defined in the cytoplasmic tails of membrane cargo that are necessary for retrograde transport. However, the precise requirements for transit from the early endosome along the retromer-dependent pathway or the Rab9-dependent pathway have not been defined. The data presented here show that furin is transported to the Golgi predominantly via the late endosomes in a Rab9- and GCC185-dependent manner, whereas TGN38 is transported directly from the early endosome to the TGN. Given that furin and TGN38 are both type 1 transmembrane proteins whose pathways diverge at the early endosome, a key question is the nature of the cargo-sorting signals that drive their segregation within this compartment. We first asked whether furin could be directed along the early-endosome-to-TGN route by replacing the tail of furin with the tail of TGN38 (FFT, Fig. 6A). At steady state, the majority of FFT was located at the Golgi (Fig. 6B). However, this Golgi localised FFT might represent either newly synthesised FFT en route to the cell surface, and/or recycling FFT. To determine the itinerary of FFT, an internalisation assay was performed with HeLa cells transfected with FFT. Significantly lower levels of FFT compared with full-length furin were trafficked to the Golgi (Fig. 7C). Rather, FFT

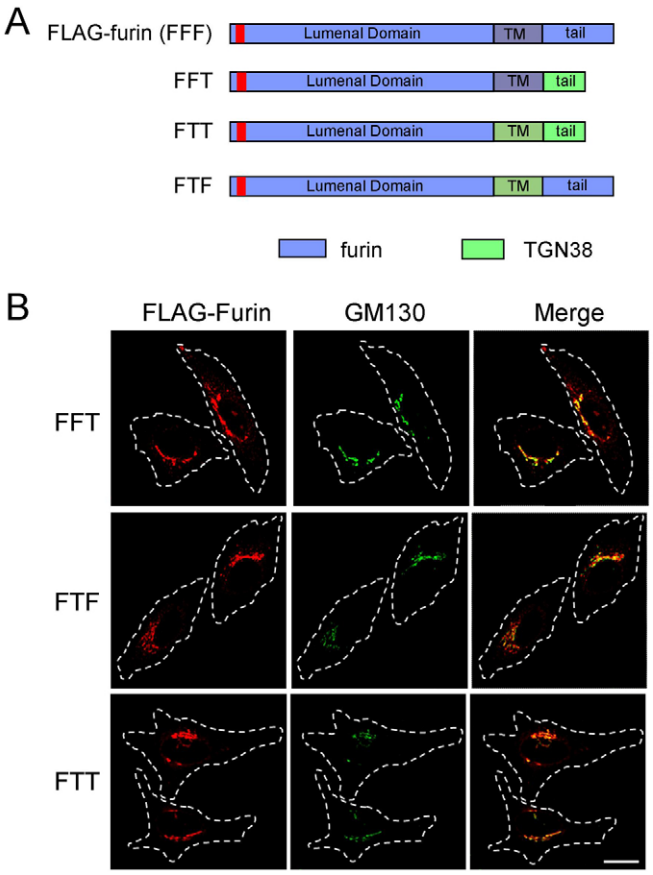

Fig. 6. Steady-state distribution of chimeric constructs of furin and TGN38 expressed in HeLa cells. (**A**) Chimeric constructs of furin (blue) and TGN38 (green) were made by piecing together the lumenal domain of furin with the transmembrane domain of furin or TGN38 and the cytoplasmic tail of furin or TGN38. The FLAG epitope is indicated by the red segment. (**B**) HeLa cells were transfected with the FFT, FTF or FTT chimeric constructs for 24 hours and fixed and permeabilised. Monolayers were stained with rabbit polyclonal anti-FLAG antibodies (red) and mouse monoclonal anti-GM130 antibodies (green). Scale bar: 10 µm.

was localised predominantly to endosomal compartments after either 60 minutes or 120 minutes of internalisation (Fig. 7A). There was significant overlap of the FFT–endosomal structures with LAMP1, indicating that FFT was transported to the late endosomes or lysosomes. The intensity of antibody–FFT staining diminished rapidly over a 120-minute period at 37°C. These data show that although FFT is predominantly transported from the cell surface to the late endosomes as for wild-type furin, it does not undergo efficient TGN retrieval and appears to be largely retained in late endosomes and lysosomes. Thus, the presence of the TGN38 cytoplasmic tail alone is not adequate to efficiently divert the furin fusion protein from the early endosome to the Golgi. The inability of FFT to be transported readily from the late endosome to the Golgi highlights the importance of the cytoplasmic tail sequence of furin in directing TGN retrieval from this compartment.

One possible explanation for the above finding is that the transmembrane domain has an important role in the segregation of cargo into distinct domains of the early endosome. Therefore, we analysed a construct containing the lumenal domain of furin fused to both the transmembrane domain and cytoplasmic tail of TGN38 (FTT, Fig. 6A). The steady state distribution of FTT showed a predominantly Golgi localisation, indicating that FTT was able to exit the ER (Fig. 6B). In contrast to FFT, internalisation assays showed that FTT was efficiently transported from the cell surface via endosomes to the Golgi over a 60-minute period (Fig. 7B,C). At 30 minutes, the FTT chimera showed very little colocalisation with CD63 (Fig. 7B), a time point where there was substantial overlap of wild-type full-length furin with CD63. Moreover, depletion of Rab9 had no impact on the transport of FTT to the Golgi (Fig. 8A–C), confirming that FTT was not using the late-endosome-to-Golgi pathway. However, knockdown of Vps26 perturbed retrograde transport of FTT (Fig. 8A,D) to a similar, if not greater, extent as it did for wild-type TGN38 (supplementary material Fig. S5), demonstrating that FTT was transported to the Golgi by a retromer-dependent pathway from early endosomes. By contrast, a furin construct containing solely the transmembrane domain of TGN38 (FTF) colocalised with CD63 after 45 minutes of internalisation and then with the Golgi at 60 minutes (supplementary material Fig. S6A,B); this finding indicates that FTF was transported to the Golgi via the late endosomes. Hence diversion of furin from the Rab9-dependent late endosome pathway to the retromer-dependent early endosome pathway required both the transmembrane domain and cytoplasmic tail of TGN38.

A possible explanation for the observed difference in trafficking of TGN38 and FTT from that of FFT is the length of the transmembrane domains of furin and TGN38. The transmembrane domain of TGN38 is slighter shorter (21 residues) than the transmembrane domain of furin (23 residues). Therefore, to explore the potential impact of the length of the transmembrane domain on endosomal trafficking, we increased the length of the transmembrane domain of TGN38 to 24 residues by the addition of three leucine or isoleucine residues in the middle of the domain (TGN38TM+3). The steady state distribution of TGN38TM+3 in transfected HeLa cells was similar to that of wtTGN38 (data not shown). However, internalisation assays showed that TGN38TM+3 was transported from the cell surface to the Golgi less efficiently than wtTGN38 (Fig. 9). At the 120-minute time point after internalisation, substantial amounts of TGN38TM+3 were associated with endosomal structures and quantification demonstrated a ~50% reduction in transport of TGN38TM+3 to the Golgi compared with wtTGN38 (Fig. 9). After 120 minutes, TGN38TM+3 was localised to EEA1-positive endosomal structures (Fig. 9), as well as additional endosomal structures, which did not appear to be labelled with late endosomal markers and could not be readily identified. These data demonstrate that the length of the transmembrane domain might be an important factor in the sorting of cargo from the early endosomes along the retrograde transport pathway.

Discussion

The intracellular trafficking of furin is relevant to the understanding of the regulation of furin activity and to providing insight on cargo sorting along the various retrograde transport pathways (Thomas, 2002). Over the past few years, considerable advances have been made in defining the routes by which membrane proteins are delivered to the TGN from the endosomal system. Multiple pathways have been defined and specific sets of machinery identified for each pathway (Lieu and Gleeson, 2011; Bonifacino and Rojas, 2006; Johannes and Popoff, 2008). Here we have investigated the itinerary of furin and defined the molecular machinery involved. First, our work has demonstrated that full-

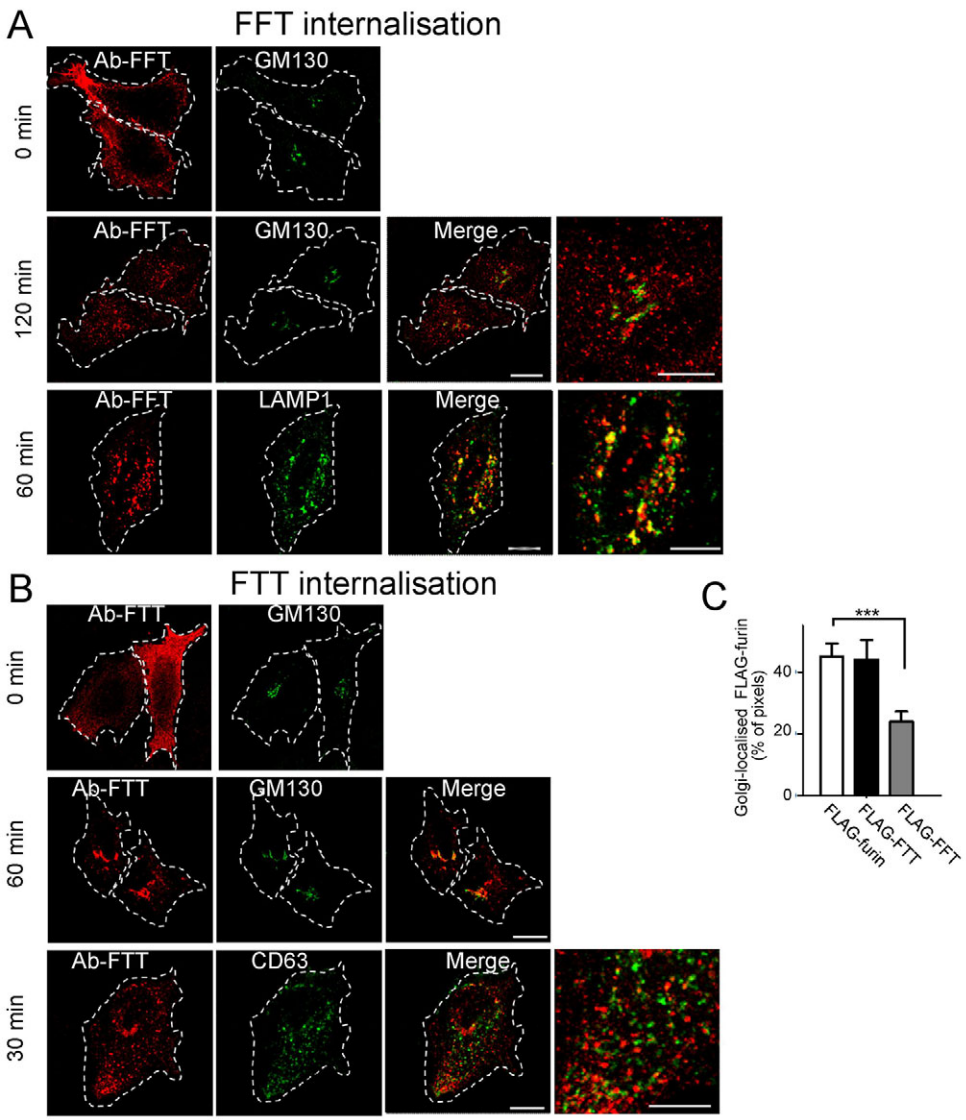

Fig. 7. Intracellular trafficking of FFT and FTT. HeLa cells were transfected with FLAG-tagged (**A**) FFT or (**B**) FTT construct for 24 hours and incubated with anti-FLAG antibodies for 45 minutes on ice followed by washes with PBS. Monolayers were either fixed and permeabilised (0 min) or incubated in serum-free media for 30, 60 minutes or 120 minutes at 37°C and then fixed and permeabilised. Monolayers were stained for the internalised antibody-bound FLAG–FFT and FLAG–FTT with Alexa-Fluor-568-conjugated anti-rabbit IgG (red) and (A) for GM130 using mouse monoclonal anti-GM130 antibodies (green) or LAMP1 using mouse monoclonal anti-LAMP1 antibodies (green) and (B) for GM130 using mouse monoclonal anti-GM130 antibodies (green) or CD63 using mouse monoclonal anti-CD63 antibodies (green). (**C**) Quantification of FLAG–FFT and FLAG–FTT levels within the Golgi. The percentage (±s.e.m.) of the total FLAG pixels that overlapped with GM130 in each cell after 60 minutes internalisation was determined using the plug-in OBCOL on ImageJ (n=20 for each sample). The data from FLAG–FFT and FLAG–FTT is expressed as a percentage of the FLAG–furin data set. ***P<0.001. Scale bars: 10 µm.

length furin is transported from the early endosome to the late endosomes and then by retrograde transport to the TGN, expanding earlier studies that used a furin chimera. Second, we have demonstrated that the efficient TGN-retrieval of furin is dependent on the GTPase Rab9 and the TGN golgin tether GCC185, which are known components of a late endosome-TGN retrograde pathway used by the M6P-R. Third, we have exploited the distinct retrograde transport pathways of furin and TGN38, and have demonstrated that efficient segregation of the two cargos at the early endosome is dependent on both the transmembrane domain and the cytoplasmic tail. And fourth, our findings indicate that the length of the transmembrane domain is a defining feature in the sorting and TGN retrieval from early endosomes.

The retrograde pathways to the TGN are now known to include a direct pathway from early endosome to the TGN, and indirect pathways via the recycling endosome or the late endosome. Hence, it was timely to expand on the early studies investigating the recycling of furin (Mallet and Maxfield, 1999). Using EEA1 and CD63 or LAMP1 as defined markers of the early and late endosomes, respectively, we have shown that the majority of furin is transported from the cell surface through the early to the late endosome during a 15–30 minute period after internalisation. Furin was not detected in substantial amounts at a Rab11-positive compartment over an extended time course, indicating that it does not transit through the recycling endosome. Because access by internalised cargo to the recycling endosome is considered to occur from the early endosome, and not the late endosome (Cullen, 2008; Johannes and Popoff, 2008), the absence of furin in the recycling endosome is consistent with the finding that the bulk of furin is transported to the late endosome.

The machinery components required for furin transport to the TGN include Rab9, GCC185 and syntaxin-10, essential components identified for the movement of M6P-R from late endosomes to the TGN (Barbero et al., 2002; Reddy et al., 2006; Ganley et al., 2008). The dependence of furin on Rab9 was demonstrated by the use of two independent siRNA targets for Rab9. Significantly, knockdown of Rab9 had no effect on the transport kinetics of TGN38, demonstrating that the block in membrane transport of furin was pathway-specific. Furin is only the second membrane cargo to be identified that uses the Rab9-dependent late endosome-to-TGN pathway. Whereas M6P-R can probably use a number of the retrograde transport pathways (Ghosh et al., 2003; Bonifacino

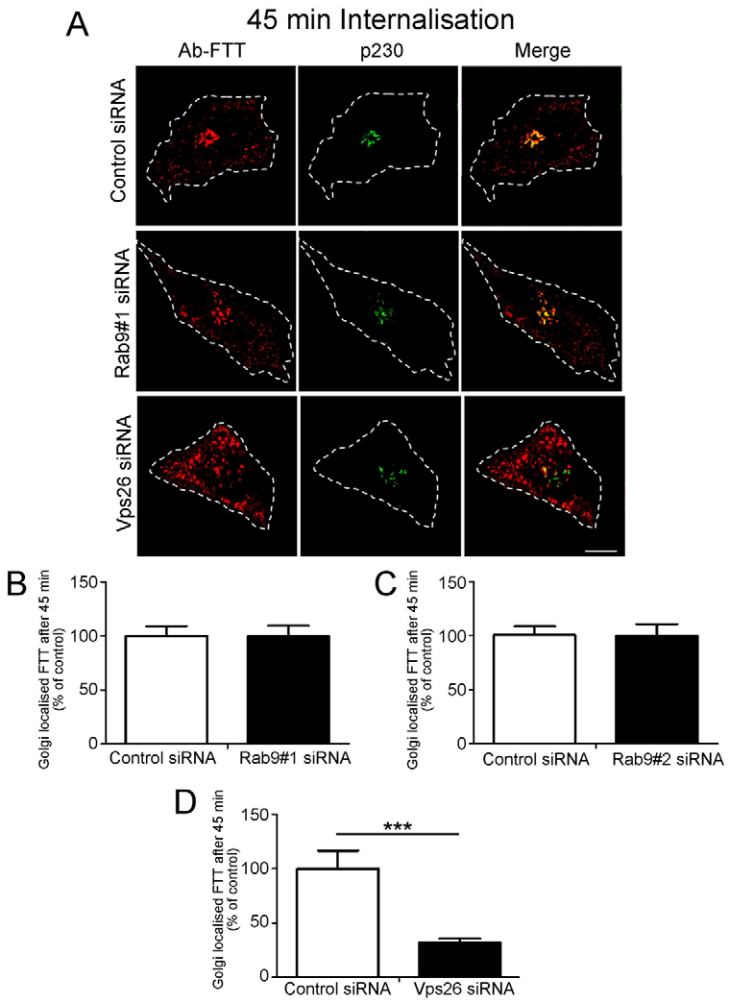

Fig. 8. Retrograde transport of FTT is Rab9 independent and Vps26 dependent. (**A**) HeLa cells were transfected with either control siRNA, Rab9#1 siRNA or siRNA to knockdown Vps26 for 48 hours and transfected again with FLAG–FTT for a further 24 hours. Monolayers were incubated with mouse anti-FLAG antibodies for 45 minutes on ice. Cells were washed in PBS and incubated in serum-free medium for 45 minutes at 37°C and then fixed and permeabilised. Monolayers were stained for the internalised antibody-bound FLAG–FTT with Alexa-Fluor-568-conjugated anti-mouse IgG (red) and for p230 with rabbit anti-p230 antibodies followed by Alexa-Fluor-488-conjugated anti-rabbit IgG (green). Scale bar: 10 µm. (**B**–**D**) Quantification of FLAG–FTT levels within the Golgi of siRNA-treated cells. The percentage of the total FLAG–FTT pixels that overlapped with p230 in each cell was determined using the plug-in OBCOL on ImageJ (n=20 for each sample). Data are expressed as a percentage (±s.e.m.) of the control siRNA data set. ***$P<0.001$.

and Rojas, 2006), the findings described here indicate that furin is primarily dependent on this late endosome pathway for transport to the TGN.

Depletion of syntaxin-10 also resulted in a defect in furin transport, with a retardation in TGN transport of furin that is similar to that reported for the M6P-R after siRNA-mediated knockdown of syntaxin-10 (Ganley et al., 2008). The dependence of furin transport on syntaxin-10 distinguishes the late-endosome-to-TGN pathway (Ganley et al., 2008) from the pathways used from the early endosomes and the recycling endosomes.

The machinery required for the transport of furin clearly distinguishes the transport of furin from TGN38. In contrast to furin, the endosome-to-TGN transport of TGN38 is independent of Rab9, GCC185 and syntaxin-10. Rather, the transport of TGN38 is retromer dependent, and conversely, the retrograde transport of furin does not require retromer. For example, depletion of Vps26, a component of the Vps26–Vps35–Vps29 retromer trimer, was effective in retarding the transport of TGN38, consistent with our previous findings (Lieu and Gleeson, 2010). Also, we have previously shown that the retrograde transport of TGN38 from early endosome is regulated by SNX2 and not SNX1 (Lieu and Gleeson, 2010), findings that are confirmed in this report. It has recently been established that there are at least four distinct retromers that differ in their sorting nexin combinations and different combinations of SNXs might be required for the endosomal sorting and transport of distinct sets of cargos (Wassmer et al., 2009).

The identification of TGN38 and furin as membrane cargo that are transported to the TGN by two distinct retrograde transport routes has provided the opportunity to identify the nature of the sorting signals responsible for the endosomal segregation of these cargos. Although various signals have been identified in the cytoplasmic tails of furin and TGN38 (Bos et al., 1993; Humphrey et al., 1993; Wong and Hong, 1993; Marks et al., 1997; Teuchert et al., 1999), and a Golgi localisation signal identified in the transmembrane domain of TGN38 (Ponnambalam et al., 1994), the relationship between the sorting motifs and the individual retrograde transport pathways have not been defined. The approach we adopted was to identify the signals required to convert a late-endosome-to-TGN cargo into an early-endosome-to-TGN cargo. We found that the cytoplasmic tail sequence of TGN38 did not efficiently divert the furin chimera (FFT) from the early endosomes to the TGN. Rather, a substantial amount of FFT was transported to the late endosome and remained in the endosomal–lysosomal pathway over extended periods. It is likely that the cytoplasmic domain of TGN38 lacks signals for transport from the late endosome to the TGN. However, inclusion of both the transmembrane domain and the cytoplasmic tail of TGN38 resulted in a furin chimera (FTT) which was efficiently transported directly from the early endosome to the TGN, a conclusion supported by the following: (1) little

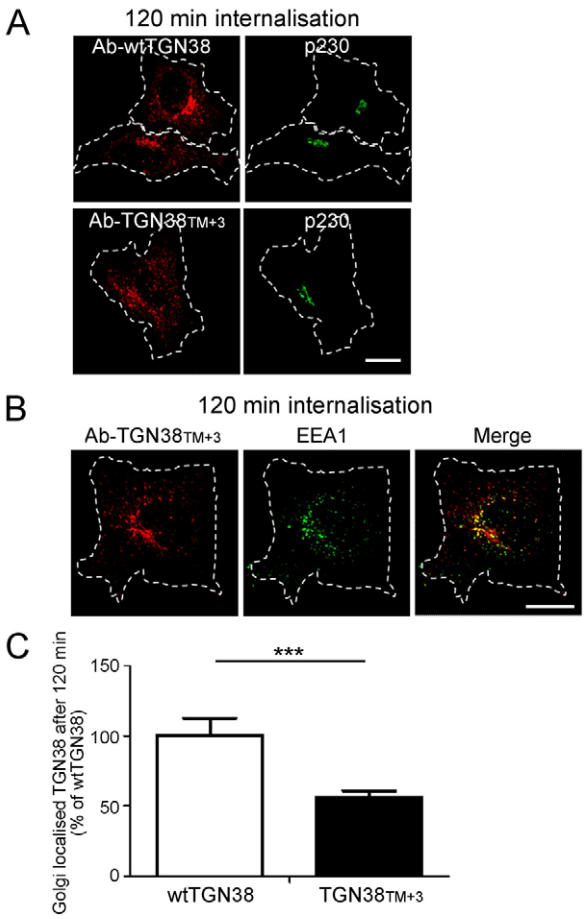

Fig. 9. Increasing the length of the transmembrane domain of TGN38 reduces the efficiency of Golgi retrieval from early endosomes. HeLa cells were transfected with full-length TGN38 (wtTGN38) or TGN38TM+3 for 24 hours. Monolayers were incubated with mouse or rabbit anti-TGN38 antibodies for 30 minutes on ice, washed in PBS and incubated in serum-free medium for 120 minutes at 37°C and then fixed and permeabilised. (**A**,**B**) The internalised antibody-bound TGN38 or TGN38TM+3 was stained with (A) Alexa-Fluor-568-conjugated anti-mouse IgG (red) and p230 using rabbit polyclonal anti-p230 antibodies (green) or (B) Alexa-Fluor-568-conjugated anti-rabbit IgG (red) and EEA1 using mouse monoclonal anti-EEA1 (green). (**C**) Quantification of TGN38TM+3 levels at the Golgi. The percentage of the total TGN38 pixels that overlapped with p230 in each cell after 120 minutes of internalisation was determined using the plug-in OBCOL on ImageJ wtTGN38. Data are expressed as a percentage (±s.e.m.) of wtTGN38 (n=35 for each sample). ***P<0.001. Scale bars: 10 µm.

colocalisation of FTT was detected with CD63 during the transport of FTT to the Golgi; (2) the retrograde transport of FTT was dependent on the retromer component Vps26; and (3) the transport of FTT was independent of Rab9. Collectively, the data indicate that FTT is transported by the same retromer-dependent route as wild-type TGN38.

Only a few studies to date have analysed the requirements for sorting and delivery from early endosomes to the TGN. The study by Reaves and co-workers (Reaves et al., 1998) is of particular relevance because they showed that both the transmembrane and cytoplasmic tail of TGN38 was required to deliver the lumenal domain of the lysosomal membrane protein Igp120 to the TGN. Replacement of the transmembrane domain of TGN38 with the transmembrane domain of Igp120 into the chimera abrogated the ability of the cytoplasmic tail of TGN38 to direct the molecule along the retrograde transport pathway (Reaves et al., 1998). The relevance of this earlier study is further enhanced by our findings comparing two cargos that use two distinct retrograde pathways.

Why does the inclusion of cargo for early-endosome-to-TGN transport depend, not only on motifs within the cytoplasmic tail, but also on the transmembrane domain? There has been considerable interest in the potential of transmembrane domains to influence the localisation of proteins (Bretscher and Munro, 1993; Simons and Ikonen, 1997; Patterson et al., 2008). Segregation of proteins into distinct lipid subdomains of the early endosome is likely to be a key factor during the endosomal sorting process and the nature of the transmembrane domain coupled with physical properties of the bilayer could be contributing factors to this process. Note that the transmembrane domain of TGN38 (21 residues) is slighter shorter than the transmembrane domain of furin (23 residues), and moreover, increasing the length of the transmembrane domain of TGN38 from 21 to 24 residues reduced its efficiency in early endosome-to-TGN transport. Indeed, a comparison of the lengths of the transmembrane domains of proteins shows that those proteins which are sorted in the early endosome for the recycling endosome and/or Golgi have transmembrane domains slightly shorter than those membrane proteins found in the late endosome or lysosome (supplementary material Table S1). A recent analysis of transmembrane domains has highlighted differences in the length of transmembrane domains of integral membrane proteins from different intracellular organelles (Sharpe et al., 2010). Sorting of membrane proteins from the early endosomes for direct transport to the Golgi requires the segregation of cargo from the vacuolar membrane of the endosome into the tubular endosomal network from which transport carriers are derived (Bonifacino and Rojas, 2006; Cullen, 2008). Based on the behaviour of lipids in model liposomes (Roux et al., 2005), the tubules emerging from the early endosome are predicted to be enriched in more mobile, less-ordered acyl chains compared with the body of the endosome, whereas the well-ordered, saturated lipids would be expected to exist as a thicker bilayer. According to the general model of lipid sorting proposed previously (Bretscher and Munro, 1993), cargo with shorter transmembrane domains could more readily enter the thinner lipid domains of the emerging tubules, whereas cargo with longer transmembrane domains would be excluded. Membrane proteins restricted to the limiting membrane of the body of the endosome would be subsequently transported to the late endosome by default. Based on this model, a combination of signals would be required to efficiently enter the retrograde pathway from the early endosome; first, a transmembrane domain which could be preferentially partitioned into the highly mobile disordered lipid domains of the tubules, and second, specific motifs in the cytoplasmic tail which can interact with retromer. The ability of FTT, but not FFT and FTF, to be efficiently sorted into the early endosome-to-TGN pathway is consistent with such a model (Fig. 10). FFT would lack a compatible transmembrane domain for efficient partitioning into the lipid bilayers of the emerging tubules and, given our finding that furin transport is retromer independent, FTF would lack a cytoplasmic tail that could interact with retromer. A mechanism involving dual signals would enhance the level of specificity in the sorting process. The reduced efficiency of early-endosome-to-TGN transport of TGN38TM+3 is consistent with this model. Clearly, the characteristics of the transmembrane domain involved in the

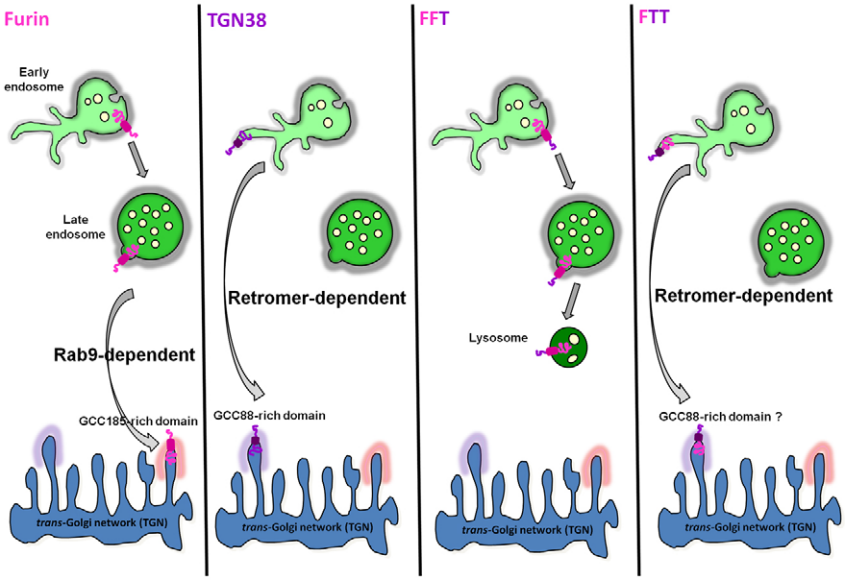

Fig. 10. Model for endosomal sorting and retrograde transport of furin chimeras. Cartoon shows the distinct retrograde pathways of furin and TGN38, with furin transported by the Rab9-dependent late-endosome-to-TGN pathway and TGN38 depicted to segregate into the tubular structures of the early endosome for retromer-dependent transport to the TGN. The sorting model proposes that furin and FFT predominantly remain in the membrane of the body of the endosome, for subsequent trafficking to the late endosome, whereas FTT is segregated into tubular domains resulting in transport to TGN. Inclusion into the tubular domains is proposed to be dependent on both the transmembrane domain and cytoplasmic tail. The TGN golgins GCC88 and GCC185 are required for retrograde transport of TGN38 (Lieu et al., 2007) and furin (herein), respectively.

sorting process, that is the relative importance of length and composition, now warrants further investigation.

An interesting issue is how such a model might accommodate the trafficking of CI-M6P-R. There is substantial evidence that CI-M6P-R requires both Rab9 and retromer for its retrieval to the Golgi (Lombardi et al., 1993; Barbero et al., 2002; Arighi et al., 2004; Seaman, 2004; Rojas et al., 2007; Ganley et al., 2008). The transport of CI-M6P-R from the cell surface to the early endosome and then to the TGN might represent a hierarchical sorting system and CI-M6P-R might be recycled by both the early-endosome-to-TGN pathway and by the late-endosome-to-TGN pathway. One general aspect that arises from the current study is the potential importance of the transmembrane domain in endosomal sorting, which needs to be considered when analysing the trafficking of reporter constructs.

In summary, this study has defined the itinerary and trafficking machinery for the retrograde transport of furin. In addition, our findings provide insight on the nature of the signals that promote cargo sorting from the early endosome along the direct retrograde transport pathway. With the other defined cargos available, there is now the opportunity to further dissect the nature of the sorting signals for specific transport by the retrograde pathways. Our findings also highlight the possibility of manipulating the precise pathway used by any one cargo to determine the physiological relevance of individual itineries.

Materials and Methods

Plasmids, antibodies and reagents

pcDNA–FLAG–furin, a furin construct containing the FLAG epitope tag inserted on the C-terminal end of the autoproteolytic maturation site of the enzyme has been described previously (Molloy et al., 1994). Rat TGN38–CFP encodes a C-terminal fusion protein with the fluorescent CFP (Keller et al., 2001). GFP–wtRab11 is an N-terminal fusion construct with GFP, as described (Zhang et al., 2004). Human autoantibodies against p230 have been previously described (Kooy et al., 1992). Rabbit and mouse anti-FLAG antibodies and anti-TGN38 antibodies were purchased from Sigma. Rabbit polyclonal antibodies against p230 (Kooy et al., 1992), GCC88 and GCC185 have been previously described (Luke et al., 2003; Derby et al., 2007). A rabbit polyclonal antibody against Vps26 was purchased from Abcam (Cambridge, UK). Rabbit polyclonal antibodies against syntaxin-16 (Mallard et al., 2002) were from Synaptic Systems (Germany) and against human syntaxin-10 were obtained from Rohan Teasdale, University of Queensland, Australia (Lieu and Gleeson, 2010). Mouse antibodies against TGN38, EEA1, GM130, syntaxin-6, SNX1 and SNX2 were from BD Biosciences (North Ryde, NSW, Australia). Mouse monoclonal antibodies against Rab9 were purchased from Abcam (Cambridge, UK) and mouse monoclonal antibodies against CD63 were from Santa Cruz Biotechnology (Santa Cruz, CA). Mouse monoclonal anti-α-tubulin was obtained from GE Healthcare (Rydalmere, NSW, Australia).

Secondary antibodies used for immunofluorescence were goat anti-rabbit IgG–Alexa-Fluor-568, goat anti-rabbit IgG–Alexa-Fluor-488, goat anti-mouse IgG–Alexa-Fluor-488, goat anti-mouse IgG–Alexa-Fluor-647, goat anti-human Alexa-Fluor-647 and goat anti-human Alexa-Fluor-568 were from Molecular Probes (Invitrogen, Carlsbad, CA). Horseradish-peroxidase-conjugated rabbit anti-goat Ig, horseradish-peroxidase-conjugated sheep anti-rabbit Ig and anti-mouse Ig were from DAKO Corporation (Carpinteria, CA).

Constructs

The FFT construct was made by first inserting a unique *Age*I site at the last codon of the transmembrane domain of pcDNA3–FLAG–furin by site-directed mutagenesis. The cytoplasmic tail of TGN38 was then amplified with *Age*I restriction sites using TGN38–CFP as a template. The resulting PCR products were digested with *Age*I and ligated. The additional bases ACCGGT from the *Age*I site were removed by site-directed mutagenesis.

The FTF construct was made via a step-wise PCR process using the FFT construct. A PCR was performed on the FFT construct using the primers, 5′-GTCCTC-TATATTGCTTACCGCTCTGGCTTTAGTTTTC-3′ and the BGH reverse primer, 5′-TAGAAGGCACAGTCGAGG-3′. This PCR product was subjected to a round of PCR using the primers, 5′-GCTGCTGTTCTTGTTGCTGTCCTCTATATTGCTTAC-3′ and the BGH reverse primer. The resulting amplified product was subjected to another round of PCR using the primers, 5′-TTCTTTGCTTATCTGGTGACCGCTGCT-GTTCTTGTTGCT-3′. A separate PCR was performed using pcDNA3-FLAG-furin as a template and the primers, 5′-CTCAGGCAGGTGTGAGGGC-3′ and the T7 primer, 5′-TAATACGACTCACTATAGGG-3′. A triple ligation was performed with the final product of the step-wise PCR, the pcDNA3–FLAG–furin PCR product and the pcDNA3 backbone using *Hin*dIII and *Nhe*I.

The FTT construct was made via step-wise PCR using the FFT construct as a template. A PCR was performed on the FFT construct using the primers, 5′-GTCCTC-TATATTGCTTACCACAACAAACGAAAGATTA-3′ and the BGH reverse primer, 5′-TAGAAGGCACAGTCGAGG-3′. This PCR product was subjected to a round of PCR using the primers, 5′-GCTGCTGTTCTTGTTGCTGTCCTCTATATTGCTTAC-3′ and the BGH reverse primer. The resulting amplified product was subjected to another round of PCR using the primers 5′-TTCTTTGCTTATCTGGTGACCGCT-GCTGTTCTTGTTGCT-3′. A separate PCR was performed using pcDNA3–FLAG–furin as a template and the primers, 5′-CTCAGGCAGGTGTGAGGGC-3′ and the T7 primer 5′-TAATACGACTCACTATAGGG-3′. A triple ligation was performed with the final product of the step-wise PCR, the pcDNA3–FLAG–furin PCR product and the pcDNA3 backbone using *Hin*dIII and *Nhe*I.

The TGN38TM+3 construct was generated by inserting the residues LLI after position 309 in the transmembrane domain of TGN38–CFP, by site-directed mutagenesis with the primers, 5′-GCCACTTCGCTTATCTGCTCCTCATCGTGAC-CGCTGCTGTTCTTGT-3′ and 5′-ACAAGAACAGCAGCGGTCACGATGAG-GAGCAGATAAGCAAAGAAGTGGC-3′.

Cell culture and transient transfections

HeLa cells were maintained as semi-confluent monolayers in Dulbecco's modified Eagle's medium (DMEM) supplemented with 10% (v/v) fetal calf serum (FCS), 2 mM L-glutamine, 100 U/µl penicillin and 0.1% (w/v) streptomycin (C-DMEM) in a humidified 10% CO_2 atmosphere at 37°C. Chinese Hamster Ovary (CHO) cells were also grown in the above medium supplemented with 40 µg/ml of L-proline. For transient transfections, HeLa cells were seeded as monolayers and transfected using Fugene 6 (Roche Diagnostics, Basel, Switzerland) according to manufacturer's instructions. Transfections were carried out in C-DMEM at 37°C, 10% CO_2 for 24–96 hours. Transient transfections with siRNA were performed using Oligofectamine (Invitrogen, Carlsbad, CA), according to manufacturer's instructions, for 72 hours prior to analyses.

RNA interference

The human GCC185 specific siRNA duplex (Reddy et al., 2006; Derby et al., 2007) and the human GCC88 specific siRNA duplex (Lieu et al., 2007) were as previously described. The siRNA against human Rab9#1 (Ganley et al., 2008), syntaxin-6 (Lieu et al., 2007), syntaxin-16 (Amessou et al., 2007) syntaxin-10 (Ganley et al., 2008), SNX1 (Carlton et al., 2004; Gullapalli et al., 2006), SNX2 (Carlton et al., 2005; Utskarpen et al., 2007) and Vps26 (Arighi et al., 2004; Popoff et al., 2007) have also been previously described. The Rab9#2 siRNA oligonucleotide is targeted to position 281–399 (GCUUCCAGAACUUAAGUAA) of the human mRNA encoding Rab9 and was designed by Sigma Proligos. All above described siRNA target sequences were purchased from Sigma Proligos (Lismore, Australia).

Indirect immunofluorescence

Cells on coverslips were fixed with 4% paraformaldehyde for 15 minutes, followed by quenching in 50 nM NH_4Cl/PBS for 10 minutes. Cells were permeabilised in 0.1% Triton X-100 in PBS for 4 minutes and blocked in 5% FCS in PBS for 20 minutes to reduce non-specific binding. Monolayers were incubated with primary and secondary conjugates as described (Kjer-Nielsen et al., 1999b) and confocal microscopy performed using a Leica TCS SP2 imaging system. Images were collected independently for multi-colour labelling.

Internalisation assays

For FLAG–furin trafficking assays, HeLa cells were transfected with siRNA for 48 hours and then transfected a second time with FLAG–furin using Fugene 6 (Roche Diagnostic) 24 hours before the internalisation assay. Mouse monoclonal or rabbit polyclonal anti-FLAG antibodies (5 µg/ml) were incubated with cells on ice for 45 minutes, cells washed, and the FLAG-antibody-bound complexes internalised for the indicated time period. Cells were then fixed with 4% paraformaldehyde according to the fixation procedure and stained with fluorochrome-conjugated secondary antibodies.

For TGN38 trafficking assays, HeLa cells were transfected with siRNA using Oligofectamine and 48 hours later, were transfected with TGN38–CFP for another 24 hours using Fugene 6. The TGN38 internalisation assays were carried out 24 hours later using either mouse monoclonal or rabbit polyclonal anti-TGN38 antibodies (1.25 µg/ml) for the indicated time period as previously described (Lieu et al., 2007).

Quantification of colocalisation

The Golgi region was defined by staining for the Golgi marker GM130 or the TGN marker p230. The early endosomes or late endosomes or lysosomes were marked with EEA1 or CD63, respectively. Quantification of the colocalisation between internalised FLAG–furin or TGN38 and organelle markers was performed using the plug-in Organelle-Based Colocalisation (OBCOL) as described previously (Woodcroft et al., 2009) on the ImageJ program (NIH public domain software) for at least 20 cells at each time point. The output is presented as a number of discrete objects found by OBCOL and the number of pixels in the Red channel (internalised FLAG–furin or TGN38) and the Green channel (endosomal, Golgi or TGN markers) found in each discrete object. The percentage of overlap with the different organelle markers was determined by taking the sum of overlapping pixels between cargo and respective markers, divided by the total number of pixels of internalised cargo within each cell. For siRNA treatment, data are presented as the percentage of the control siRNA dataset. All analyses included samples from two or more independent experiments.

Immunoblotting

Cell extracts were dissolved in reducing sample buffer and samples were resolved on a 4–12% NuPAGE pre-cast gradient gel and immunoblotting was performed as described (Lieu et al., 2007). Analysis of images was performed using the Gel Pro Analyzer program (MediaCybernetics, Bethesda, MD).

Statistical analyses

Data obtained from fluorescence intensity of Golgi-localised antibody–furin or antibody–TGN38 complexes was expressed as the mean ± s.e.m. and analysed by an unpaired, two-tailed, Student's *t*-test using GraphPad Prism version 5.00 for Windows, GraphPad software, San Diego, CA. A value of $*P<0.05$ was considered as significant, $**P<0.01$ was highly significant and $***P<0.001$ was very highly significant. The absence of a *P* value indicates a non-significant difference.

We gratefully thank Gary Thomas for the full-length furin construct and Fiona Houghton for expert technical advice. This work was supported by funding from the National Health and Medical Research Council of Australia. P.Z.C.C. is supported by a Melbourne International Graduate Scholarship.

Supplementary material available online at
http://jcs.biologists.org/cgi/content/full/124/14/2401/DC1

References

Amessou, M., Fradagrada, A., Falguieres, T., Lord, J. M., Smith, D. C., Roberts, L. M., Lamaze, C. and Johannes, L. (2007). Syntaxin 16 and syntaxin 5 are required for efficient retrograde transport of several exogenous and endogenous cargo proteins. *J. Cell Sci.* **120**, 1457-1468.

Arighi, C. N., Hartnell, L. M., Aguilar, R. C., Haft, C. R. and Bonifacino, J. S. (2004). Role of the mammalian retromer in sorting of the cation-independent mannose 6-phosphate receptor. *J. Cell Biol.* **165**, 123-133.

Banting, G. and Ponnambalam, S. (1997). TGN38 and its orthologues: roles in post-TGN vesicle formation and maintenance of TGN morphology. *Biochim. Biophys. Acta* **1355**, 209-217.

Banting, G., Maile, R. and Roquemore, E. P. (1998). The steady state distribution of humTGN46 is not significantly altered in cells defective in clathrin-mediated endocytosis. *J. Cell Sci.* **111**, 3451-3458.

Barbero, P., Bittova, L. and Pfeffer, S. R. (2002). Visualization of Rab9-mediated vesicle transport from endosomes to the trans-Golgi in living cells. *J. Cell Biol.* **156**, 511-518.

Barr, F. A. (1999). A novel Rab6-interacting domain defines a family of Golgi-targeted coiled-coil proteins. *Curr. Biol.* **9**, 381-384.

Belenkaya, T. Y., Wu, Y., Tang, X., Zhou, B., Cheng, L., Sharma, Y. V., Yan, D., Selva, E. M. and Lin, X. (2008). The retromer complex influences Wnt secretion by recycling wntless from endosomes to the trans-Golgi network. *Dev. Cell* **14**, 120-131.

Bennett, B. D., Denis, P., Haniu, M., Teplow, D. B., Kahn, S., Louis, J. C., Citron, M. and Vassar, R. (2000). A furin-like convertase mediates propeptide cleavage of BACE, the Alzheimer's beta-secretase. *J. Biol. Chem.* **275**, 37712-37717.

Bonifacino, J. S. and Rojas, R. (2006). Retrograde transport from endosomes to the trans-Golgi network. *Nat. Rev. Mol. Cell Biol.* **7**, 568-579.

Bos, K., Wraight, C. and Stanley, K. K. (1993). TGN38 is maintained in the trans-Golgi network by a tyrosine-containing motif in the cytoplasmic domain. *EMBO J.* **12**, 2219-2228.

Braulke, T. and Bonifacino, J. S. (2009). Sorting of lysosomal proteins. *Biochim. Biophys. Acta* **1793**, 605-614.

Bretscher, M. S. and Munro, S. (1993). Cholesterol and the Golgi apparatus. *Science* **261**, 1280-1281.

Bujny, M. V., Popoff, V., Johannes, L. and Cullen, P. J. (2007). The retromer component sorting nexin-1 is required for efficient retrograde transport of Shiga toxin from early endosome to the trans Golgi network. *J. Cell Sci.* **120**, 2010-2021.

Caporaso, G. L., Takei, K., Gandy, S. E., Matteoli, M., Mundigl, O., Greengard, P. and De Camilli, P. (1994). Morphologic and biochemical analysis of the intracellular trafficking of the Alzheimer beta/A4 amyloid precursor protein. *J. Neurosci.* **14**, 3122-3138.

Carlton, J., Bujny, M., Peter, B. J., Oorschot, V. M., Rutherford, A., Mellor, H., Klumperman, J., McMahon, H. T. and Cullen, P. J. (2004). Sorting nexin-1 mediates tubular endosome-to-TGN transport through coincidence sensing of high- curvature membranes and 3-phosphoinositides. *Curr. Biol.* **14**, 1791-1800.

Carlton, J. G., Bujny, M. V., Peter, B. J., Oorschot, V. M., Rutherford, A., Arkell, R. S., Klumperman, J., McMahon, H. T. and Cullen, P. J. (2005). Sorting nexin-2 is associated with tubular elements of the early endosome, but is not essential for retromer-mediated endosome-to-TGN transport. *J. Cell Sci.* **118**, 4527-4539.

Cui, Y., Jean, F., Thomas, G. and Christian, J. L. (1998). BMP-4 is proteolytically activated by furin and/or PC6 during vertebrate embryonic development. *EMBO J.* **17**, 4735-4743.

Cullen, P. J. (2008). Endosomal sorting and signalling: an emerging role for sorting nexins. *Nat. Rev. Mol. Cell Biol.* **9**, 574-582.

Derby, M. C., Lieu, Z. Z., Brown, D., Stow, J. L., Goud, B. and Gleeson, P. A. (2007). The trans-Golgi network golgin, GCC185, is required for endosome-to-Golgi transport and maintenance of Golgi structure. *Traffic* **8**, 758-773.

Dubois, C. M., Blanchette, F., Laprise, M. H., Leduc, R., Grondin, F. and Seidah, N. G. (2001). Evidence that furin is an authentic transforming growth factor-beta1-converting enzyme. *Am. J. Pathol.* **158**, 305-316.

Franch-Marro, X., Wendler, F., Guidato, S., Griffith, J., Baena-Lopez, A., Itasaki, N., Maurice, M. M. and Vincent, J. P. (2008). Wingless secretion requires endosome-to-Golgi retrieval of Wntless/Evi/Sprinter by the retromer complex. *Nat. Cell Biol.* **10**, 170-177.

Ganley, I. G., Espinosa, E. and Pfeffer, S. R. (2008). A syntaxin 10-SNARE complex distinguishes two distinct transport routes from endosomes to the trans-Golgi in human cells. *J. Cell Biol.* **180**, 159-172.

Ghosh, P., Dahms, N. M. and Kornfeld, S. (2003). Mannose 6-phosphate receptors: new twists in the tale. *Nat. Rev. Mol. Cell Biol.* **4**, 202-212.

Ghosh, R. N., Mallet, W. G., Soe, T. T., McGraw, T. E. and Maxfield, F. R. (1998). An endocytosed TGN38 chimeric protein is delivered to the TGN after trafficking through the endocytic recycling compartment in CHO cells. *J. Cell Biol.* **142**, 923-936.

Goldstein, J. L., Anderson, R. G. and Brown, M. S. (1979). Coated pits, coated vesicles, and receptor-mediated endocytosis. *Nature* **279**, 679-685.

Goud, B. and Gleeson, P. A. (2010). TGN golgins, Rabs and cytoskeleton: regulating the Golgi trafficking highways. *Trends Cell Biol.* **20**, 329-336.
Grant, B. D. and Donaldson, J. G. (2009). Pathways and mechanisms of endocytic recycling. *Nat. Rev. Mol. Cell. Biol.* **10**, 597-608.
Gullapalli, A., Wolfe, B. L., Griffin, C. T., Magnuson, T. and Trejo, J. (2006). An essential role for SNX1 in lysosomal sorting of protease-activated receptor-1: evidence for retromer-, Hrs-, and Tsg101-independent functions of sorting nexins. *Mol. Biol. Cell* **17**, 1228-1238.
He, X., Li, F., Chang, W. P. and Tang, J. (2005). GGA proteins mediate the recycling pathway of memapsin 2 (BACE). *J. Biol. Chem.* **280**, 11696-11703.
Humphrey, J. S., Peters, P. J., Yuan, L. C. and Bonifacino, J. S. (1993). Localization of TGN38 to the trans-Golgi network: involvement of a cytoplasmic tyrosine-containing sequence. *J. Cell Biol.* **120**, 1123-1135.
Johannes, L. and Popoff, V. (2008). Tracing the retrograde route in protein trafficking. *Cell* **135**, 1175-1187.
Keller, P., Toomre, D., Diaz, E., White, J. and Simons, K. (2001). Multicolour imaging of post-Golgi sorting and trafficking in live cells. *Nat. Cell Biol.* **3**, 140-149.
Kinoshita, A., Fukumoto, H., Shah, T., Whelan, C. M., Irizarry, M. C. and Hyman, B. T. (2003). Demonstration by FRET of BACE interaction with the amyloid precursor protein at the cell surface and in early endosomes. *J. Cell Sci.* **116**, 3339-3346.
Kjer-Nielsen, L., Teasdale, R. D., van Vliet, C. and Gleeson, P. A. (1999a). A novel Golgi-localisation domain shared by a class of coiled-coil peripheral membrane proteins. *Curr. Biol.* **9**, 385-388.
Kjer-Nielsen, L., van Vliet, C., Erlich, R., Toh, B. H. and Gleeson, P. A. (1999b). The Golgi-targeting sequence of the peripheral membrane protein p230. *J. Cell Sci.* **112**, 1645-1654.
Kooy, J., Toh, B. H., Pettitt, J. M., Erlich, R. and Gleeson, P. A. (1992). Human autoantibodies as reagents to conserved Golgi components – Characterization of a peripheral, 230-kDa compartment-specific Golgi protein. *J. Biol. Chem.* **267**, 20255-20263.
Lieu, Z. Z. and Gleeson, P. A. (2010). Identification of different itineraries and retromer components for endosome-to-Golgi transport of TGN38 and Shiga toxin. *Eur. J. Cell Biol.* **89**, 379-393.
Lieu, Z. Z. and Gleeson, P. A. (2011). Endosome-to-Golgi transport pathways in physiological processes. *Histol. Histopathol.* **26**, 395-408.
Lieu, Z. Z., Derby, M. C., Teasdale, R. D., Hart, C., Gunn, P. and Gleeson, P. A. (2007). The Golgin, GCC88, is required for efficient retrograde transport of cargo from the early endosomes to the trans-Golgi network. *Mol. Biol. Cell* **18**, 4979-4991.
Lombardi, D., Soldati, T., Riederer, M. A., Goda, Y., Zerial, M. and Pfeffer, S. R. (1993). Rab9 functions in transport between late endosomes and the trans Golgi network. *EMBO J.* **12**, 677-682.
Lopez-Perez, E., Zhang, Y., Frank, S. J., Creemers, J., Seidah, N. and Checler, F. (2001). Constitutive alpha-secretase cleavage of the beta-amyloid precursor protein in the furin-deficient LoVo cell line: involvement of the pro-hormone convertase 7 and the disintegrin metalloprotease ADAM10. *J. Neurochem.* **76**, 1532-1539.
Luke, M. R., Kjer-Nielsen, L., Brown, D. L., Stow, J. L. and Gleeson, P. A. (2003). GRIP domain-mediated targeting of two new coiled-coil proteins, GCC88 and GCC185, to subcompartments of the trans-Golgi network. *J. Biol. Chem.* **278**, 4216-4226.
Mallard, F., Antony, C., Tenza, D., Salamero, J., Goud, B. and Johannes, L. (1998). Direct pathway from early/recycling endosomes to the Golgi apparatus revealed through the study of shiga toxin B-fragment transport. *J. Cell Biol.* **143**, 973-990.
Mallard, F., Tang, B. L., Galli, T., Tenza, D., Saint-Pol, A., Yue, X., Antony, C., Hong, W., Goud, B. and Johannes, L. (2002). Early/recycling endosomes-to-TGN transport involves two SNARE complexes and a Rab6 isoform. *J. Cell Biol.* **156**, 653-664.
Mallet, W. G. and Maxfield, F. R. (1999). Chimeric forms of furin and TGN38 are transported with the plasma membrane in the trans-Golgi network via distinct endosomal pathways. *J. Cell Biol.* **146**, 345-359.
Marks, M. S., Ohno, H., Kirchhausen, T. and Bonifacino, S. J. (1997). Protein sorting by tyrosine-based signals: adapting to the Ys and wherefores. *Trends Cell Biol.* **7**, 124-128.
Molloy, S. S., Anderson, E. D., Jean, F. and Thomas, G. (1999). Bi-cycling the furin pathway: from TGN localization to pathogen activation and embryogenesis. *Trends Cell Biol.* **9**, 28-35.
Molloy, S. S., Bresnahan, P. A., Leppla, S. H., Klimpel, K. R. and Thomas, G. (1992). Human furin is a calcium-dependent serine endoprotease that recognizes the sequence Arg-X-X-Arg and efficiently cleaves anthrax toxin protective antigen. *J. Biol. Chem.* **267**, 16396-16402.
Molloy, S. S., Thomas, L., Vanslyke, J. K., Stenberg, P. E. and Thomas, G. (1994). Intracellular trafficking and activation of the furin proprotein Convertase-Localization to the Tgn and recycling from the cell surface. *EMBO J.* **13**, 18-33.
Munro, S. and Nichols, B. J. (1999). The GRIP domain- a novel Golgi-targeting domain found in several coiled-coil proteins. *Curr. Biol.* **9**, 377-380.
Nielsen, M. S., Gustafsen, C., Madsen, P., Nyengaard, J. R., Hermey, G., Bakke, O., Mari, M., Schu, P., Pohlmann, R., Dennes, A. et al. (2007). Sorting by the cytoplasmic domain of the amyloid precursor protein binding receptor SorLA. *Mol. Cell Biol.* **27**, 6842-6851.
Patterson, G. H., Hirschberg, K., Polishchuk, R. S., Gerlich, D., Phair, R. D. and Lippincott-Schwartz, J. (2008). Transport through the Golgi apparatus by rapid partitioning within a two-phase membrane system. *Cell* **133**, 1055-1067.
Plaut, R. D. and Carbonetti, N. H. (2008). Retrograde transport of pertussis toxin in the mammalian cell. *Cell. Microbiol.* **10**, 1130-1139.
Ponnambalam, S., Rabouille, C., Luzio, J. P., Nilsson, T. and Warren, G. (1994). The TGN38 glycoprotein contains two non-overlapping signals that mediate localization to the trans-Golgi network. *J. Cell Biol.* **125**, 253-268.
Popoff, V., Mardones, G. A., Tenza, D., Rojas, R., Lamaze, C., Bonifacino, J. S., Raposo, G. and Johannes, L. (2007). The retromer complex and clathrin define an early endosomal retrograde exit site. *J. Cell Sci.* **120**, 2022-2031.
Port, F., Kuster, M., Herr, P., Furger, E., Banziger, C., Hausmann, G. and Basler, K. (2008). Wingless secretion promotes and requires retromer-dependent cycling of Wntless. *Nat. Cell Biol.* **10**, 178-185.
Reaves, B. J., Banting, G. and Luzio, J. P. (1998). Lumenal and transmembrane domains play a role in sorting type I membrane proteins on endocytic pathways. *Mol. Biol. Cell* **9**, 1107-1122.
Reddy, J. V., Burguete, A. S., Sridevi, K., Ganley, I. G., Nottingham, R. M. and Pfeffer, S. R. (2006). A functional role for the GCC185 golgin in mannose 6-phosphate receptor recycling. *Mol. Biol. Cell* **17**, 4353-4363.
Rojas, R., Kametaka, S., Haft, C. R. and Bonifacino, J. S. (2007). Interchangeable but essential functions of SNX1 and SNX2 in the association of retromer with endosomes and the trafficking of mannose 6-phosphate receptors. *Mol. Cell. Biol.* **27**, 1112-1124.
Roquemore, E. P. and Banting, G. (1998). Efficient trafficking of TGN38 from the endosome to the trans-Golgi network requires a free hydroxyl group at position 331 in the cytosolic domain. *Mol. Biol. Cell* **9**, 2125-2144.
Roux, A., Cuvelier, D., Nassoy, P., Prost, J., Bassereau, P. and Goud, B. (2005). Role of curvature and phase transition in lipid sorting and fission of membrane tubules. *EMBO J.* **24**, 1537-1545.
Saftig, P. and Klumperman, J. (2009). Lysosome biogenesis and lysosomal membrane proteins: trafficking meets function. *Nat. Rev. Mol. Cell. Biol.* **10**, 623-635.
Sandvig, K. and van Deurs, B. (2000). Entry of ricin and Shiga toxin into cells: molecular mechanisms and medical perspectives. *EMBO J.* **19**, 5943-5950.
Sandvig, K. and van Deurs, B. (2005). Delivery into cells: lessons learned from plant and bacterial toxins. *Gene Ther.* **12**, 865-872.
Seaman, M. N. (2004). Cargo-selective endosomal sorting for retrieval to the Golgi requires retromer. *J. Cell Biol.* **165**, 111-122.
Seaman, M. N. (2005). Recycle your receptors with retromer. *Trends Cell Biol.* **15**, 68-75.
Sharpe, H. J., Stevens, T. J. and Munro, S. (2010). A comprehensive comparison of transmembrane domains reveals organelle-specific properties. *Cell* **142**, 158-169.
Shewan, A. M., van Dam, E. M., Martin, S., Luen, T. B., Hong, W., Bryant, N. J. and James, D. E. (2003). GLUT4 recycles via a trans-Golgi network (TGN) subdomain enriched in Syntaxins 6 and 16 but not TGN38: involvement of an acidic targeting motif. *Mol. Biol. Cell* **14**, 973-986.
Simons, K. and Ikonen, E. (1997). Functional rafts in cell membranes. *Nature* **387**, 569-572.
Teuchert, M., Berghofer, S., Klenk, H. D. and Garten, W. (1999). Recycling of furin from the plasma membrane-Functional importance of the cytoplasmic tail sorting signals and interaction with the AP-2 adaptor medium chain subunit. *J. Biol. Chem.* **274**, 36781-36789.
Thomas, G. (2002). Furin at the cutting edge: from protein traffic to embryogenesis and disease. *Nat. Rev. Mol. Cell Biol.* **3**, 753-766.
Tran, T. H., Zeng, Q. and Hong, W. (2007). VAMP4 cycles from the cell surface to the trans-Golgi network via sorting and recycling endosomes. *J. Cell Sci.* **120**, 1028-1041.
Utskarpen, A., Slagsvold, H. H., Iversen, T. G., Walchli, S. and Sandvig, K. (2006). Transport of ricin from endosomes to the Golgi apparatus is regulated by Rab6A and Rab6A'. *Traffic* **7**, 663-672.
Utskarpen, A., Slagsvold, H. H., Dyve, A. B., Skanland, S. S. and Sandvig, K. (2007). SNX1 and SNX2 mediate retrograde transport of Shiga toxin. *Biochem. Biophys. Res. Commun.* **358**, 566-570.
Verges, M., Luton, F., Gruber, C., Tiemann, F., Reinders, L. G., Huang, L., Burlingame, A. L., Haft, C. R. and Mostov, K. E. (2004). The mammalian retromer regulates transcytosis of the polymeric immunoglobulin receptor. *Nat. Cell Biol.* **6**, 763-769.
Voorhees, P., Deignan, E., Vandonselaar, E., Humphrey, J., Marks, M. S., Peters, P. J. and Bonifacino, J. S. (1995). An acidic sequence within the cytoplasmic domain of furin functions as a determinant of trans-Golgi network localization and internalization from the cell surface. *EMBO J.* **14**, 4961-4975.
Wassmer, T., Attar, N., Harterink, M., van Weering, J. R., Traer, C. J., Oakley, J., Goud, B., Stephens, D. J., Verkade, P., Korswagen, H. C. et al. (2009). The retromer coat complex coordinates endosomal sorting and dynein-mediated transport, with carrier recognition by the trans-Golgi network. *Dev. Cell* **17**, 110-122.
Wang, X., Ma, D., Keski-Oja, J. and Pei, D. (2004). Co-recycling of MT1-MMP and MT3-MMP through the trans-Golgi network. Identification of DKV582 as a recycling signal. *J. Biol. Chem.* **279**, 9331-9336.
Wong, S. H. and Hong, W. J. (1993). The SXYQRL sequence in the cytoplasmic domain of TGN38 plays a major role in trans-Golgi network localization. *J. Biol. Chem.* **268**, 22853-22862.
Woodcroft, B. J., Hammond, L., Stow, J. L. and Hamilton, N. A. (2009). Automated organelle-based colocalization in whole-cell imaging. *Cytometry A* **75**, 941-950.
Xu, Y., Martin, S., James, D. E. and Hong, W. (2002). GS15 forms a SNARE complex with syntaxin 5, GS28, and Ykt6 and is implicated in traffic in the early cisternae of the Golgi apparatus. *Mol. Biol. Cell* **13**, 3493-3507.
Yang, P. T., Lorenowicz, M. J., Silhankova, M., Coudreuse, D. Y., Betist, M. C. and Korswagen, H. C. (2008). Wnt signaling requires retromer-dependent recycling of MIG-14/Wntless in Wnt-producing cells. *Dev. Cell* **14**, 140-147.
Zhang, X. M., Ellis, S., Sriratana, A., Mitchell, C. A. and Rowe, T. (2004). Sec15 is an effector for the Rab11 GTPase in mammalian cells. *J. Biol. Chem.* **279**, 43027-43034.

Journal of Cell Science